Applied Catalysis B: Environmental 111–112 (2012) 636–640

Contents lists available at SciVerse ScienceDirect

Applied Catalysis B: Environmental

journal homepage: www.elsevier.com/locate/apcatb

Reaction mechanism of visible-light responsive Cu(II)-grafted Mo-doped $SrTiO_3$ photocatalyst studied by means of ESR spectroscopy and chemiluminescence photometry

Yoshio Nosaka[a,*], Shinichiro Takahashi[a], Yasufumi Mitani[a], Xiaoqing Qiu[b], Masahiro Miyauchi[c]

[a] Department of Materials Science and Technology, Nagaoka University of Technology, Nagaoka-shi, Niigata 940-2188, Japan
[b] Research Center for Advanced Science and Technology, The University of Tokyo, 4-6-1, Komaba, Meguro-ku, Tokyo 153-8904, Japan
[c] Department of Metallurgy and Ceramics Science, Tokyo Institute of Technology, 2-12-1, Ookayama, Meguro-ku, Tokyo 152-8552, Japan

ARTICLE INFO

Article history:
Received 2 October 2011
Received in revised form 5 November 2011
Accepted 8 November 2011
Available online 18 November 2011

Keywords:
Visible light responsive photocatalyst
Mo doped $SrTiO_3$
Cu(II) graft
ESR
Superoxide radical

ABSTRACT

The reaction mechanisms of visible-light responsive Cu(II)-grafted Mo-doped $SrTiO_3$ (Cu(II)/MoSTO) photocatalyst and related photocatalysts were analyzed by means of ESR spectroscopy for detecting trapped carriers at 77 K and chemiluminescence photometry for $O_2^{\bullet-}$ and H_2O_2 in aqueous suspension. On the irradiation of visible light, the reduction of grafted Cu^{2+} ions was observed by ESR measurements for both Cu(II)/MoSTO and Cu(II)/STO (Cu(II)-grafted undoped $SrTiO_3$) photocatalysts. One electron reduction product for O_2, i.e., $O_2^{\bullet-}$, was detected in aqueous suspension by 442-nm irradiation for the Cu(II)-grafted samples. On the other hand, the amount of H_2O_2 detected as the two electron reduction product of O_2 was a very small scale, indicating possible further reduction of H_2O_2 into H_2O. From the ESR observations of crystalline defects, it was concluded that the Mo doping to increase visible-light response also increase the electron–hole recombination to some extent, while the Cu(II) grafting functioned as a trap of excited electrons to decrease the recombination.

1. Introduction

Photocatalytic reactions with metal oxide semiconductors represented by TiO_2 have been attracting much attention in view of their practical applications to environmental cleaning such as self cleaning of tiles, glasses, and windows [1–4]. A serious disadvantage of TiO_2 would be that only UV light can be utilized for photocatalytic reactions and the application fields are restricted to out-door products or purification filters. Therefore, it is of great interest to design new materials (or composites) to extend the range of absorption wavelength to visible region. Several groups have been succeeded in doping nitrogen [5–8] and sulfur [9–11] to TiO_2 for extending the absorption wavelength. However, when valence band of TiO_2 was raised by doping, the oxidation ability become lower than the undoped TiO_2. For example, N-doped TiO_2 was not enough to decompose acetaldehyde to CO_2 [12,13]. Then the modification for conduction band to narrow the band gap is favorable for high oxidation power. Irie et al. [14] designed and fabricated Cu(II)-grafted TiO_2 where the excitation of interfacial charge transfer (IFCT) band directly induces Cu^+ which can reduce O_2 to H_2O_2 with two electrons. Since the magnitude of IFCT absorbance is small, Miyauchi and coworkers [15] succeeded to form an energy level under conduction band for effective absorption of visible light by doping of Mo^{6+} and Na^+ into $SrTiO_3$. Although the doping of transition metal ions into TiO_2 may be also photocatalytically active in visible region and many researches have been reported [16–18], $SrTiO_3$ is suitable to be doped for metal ions because of the perovskite structure [15].

As for the reactive intermediates in photocatalysis, trapped holes and electrons, $O_2^{\bullet-}$ are important species [3]. Besides, H_2O_2 which will be formed by multi-electron reduction of O_2 at grafted Cu(II) is an important species to understand the visible-light induced reaction for the photocatalysts of Cu(II)-grafted metal oxides. We have been analyzing the TiO_2 photocatalysis by monitoring $O_2^{\bullet-}$ [19–21], H_2O_2 [20,21] and trapped electrons and holes [22] so far. Then, in the present study these analytical methods were applied for clarifying the mechanism of photocatalytic efficiency of Cu(II)-grafted Mo-doped $SrTiO_3$ photocatalyst. As the result, we succeeded to clarify the characteristics of visible-light induced photocatalytic reactions for the modified $SrTiO_3$ photocatalysts.

* Corresponding author. Tel.: +81 258 47 9315; fax: +81 258 47 9315.
E-mail address: nosaka@nagaokaut.ac.jp (Y. Nosaka).

0926-3373/$ – see front matter © 2011 Elsevier B.V. All rights reserved.
doi:10.1016/j.apcatb.2011.11.017

2. Experimental

2.1. Materials

Molybdenum-doped strontium titanate (MoSTO) used in the present report was prepared by hydrothermal method from the mixture of $Sr(OH)_2$, amorphous TiO_2 and Na_2MoO_4 as reported in the previous paper [15]. The components of the MoSTO sample was $(Sr_{0.9975}Na_{0.0025})(Ti_{0.98}Mo_{0.02})O_3$. Undoped strontium titanate (STO) used was prepared by the same method. Modification of Cu(II) ions to STO and MoSTO was done with $CuCl_2$ solution according to the literature [14,15]. The amount of Cu(II) in Cu(II)/STO and Cu(II)/MoSTO samples used in the present study was 0.1 wt% [15].

Luminol (Nacalai Tesqu, Inc.) as a chemiluminescence probe and hemoglobin (Hb) from bovine (Wako Pure Chemical Industries, Inc.), were used without further purification. The water used was distilled followed by purification with a Milli-Q system.

2.2. Electron spin resonance (ESR) spectroscopy

For the ESR measurements, 20 mg of the photocatalyst powder was placed in a quartz sample tube (5 mm O.D.) with a Young vacuum joint and a stop cock, and then it was evacuated by a rotary pump and closed. The measurements were performed at 77 K with a JEOL ES-RE2X ESR spectrometer under photo-irradiation with a 500 W mercury lamp (Ushio, USH 500D). One of the three kinds of glass filters, a 360 nm band-pass filter (Toshiba UV-D36C) and sharp cut filters (HOYA, L42 and Y50) was inserted in the light path. The UV band-pass filter transmits only 365-nm line of the mercury lamp. While the Y50 filter transmits 550- and 580-nm lines (>500 nm), the L42 filter transmits all visible light containing 436-nm line (>420 nm). In the ESR measurements, experimental conditions were the microwave frequency of 9.13 GHz, microwave power of 10 mW, and the field modulation of 1 mT. The six signal lines of a Mn^{2+} marker recorded with samples were used to scale *g*-values in the spectra. To demonstrate the effect of photoirradiation on the ESR spectra, a difference spectrum was calculated by subtracting the spectrum obtained in the dark.

2.3. Luminol chemiluminescence (CL) probe method

The formation of $O_2^{\bullet -}$ was observed by using luminol CL probe method [19,20] as follows. Into a 1 cm × 1 cm quartz cell containing 3.5 mL of 0.01 M NaOH solution, 15 mg of photocatalyst powder was added. The cell was placed in a dark box and the side face of the cell was irradiated with a He-Cd laser (442 nm, 14 mW cm^{-2}, KIMMON Inc., IK5652R-G). After laser irradiation, 50 μL of 7 mM luminol solution (0.01 M NaOH) was immediately injected by a micro syringe into the suspension. The CL intensity was measured with a Peltier-cooled photon-counter head (Hamamatsu, H7421) and the counted number of photons was integrated over 100 s. Other details in the apparatus and the CL reaction have been described previously [20].

The experimental procedure for the selective detection of H_2O_2 is basically similar to the $O_2^{\bullet -}$ measurement except for the injection solution and the timing. After the luminol injection, Hb solution was injected into the suspension and the time profile of the CL intensity was measured. The observed CL intensity can be converted to H_2O_2 concentration as have been reported previously in details [21].

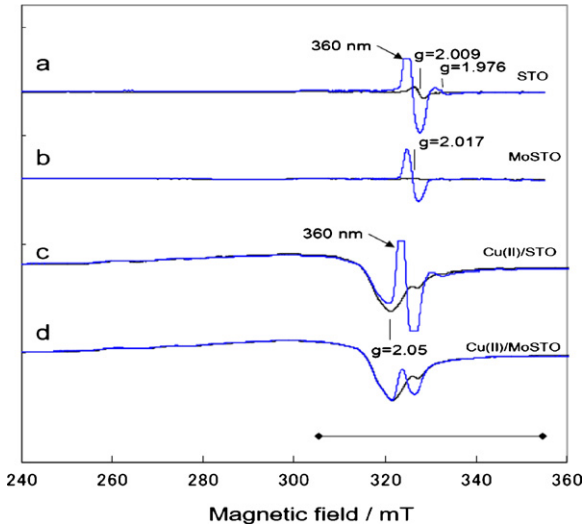

Fig. 1. ESR spectra of modified $SrTiO_3$ systems measured at 77 K under vacuum and the effect of UV irradiation. The horizontal bar shows the range of magnetic filed for the expanded differential spectra in Fig. 2.

3. Results and discussion

3.1. ESR analysis

Fig. 1 shows ESR spectra and the effect of UV irradiation for modified $SrTiO_3$ photocatalysts, i.e., (a); $SrTiO_3$, (b); Mo-doped $SrTiO_3$, (c); Cu(II)-grafted $SrTiO_3$, and (d); Cu(II)-grafted Mo-doped $SrTiO_3$, which were denoted as STO, MoSTO. Cu(II)/STO, and Cu(II)/MoSTO, respectively. The large signal observed under dark for Cu(II)-grafted samples (spectra c and d) in the magnetic field region of 260–330 mT is attributable to Cu^{2+}. The Cu^{2+} signal was broad comparing to that on Cu(II) doped TiO_2 [23], suggesting that the chemical structure around Cu^{2+} is not homogeneous. The $SrTiO_3$ sample gave the ESR signal at $g = 2.009$ before the irradiation (spectrum a), whose *g*-value corresponds to that of oxygen vacancy or crystalline defects. The assignment to lattice vacancy is supported by the fact that this signal was decreased by Mo doping (spectrum b). It is noted that the formation of oxygen vacancies is retarded in MoSTO, even though it is doped with transition metal ions into STO crystal. In the MoSTO, sodium ions (Na^+) are also doped as well as Mo^{6+} to compensate the charge balance in the crystal [15], thus the formation of oxygen vacancies in MoSTO is decreased as compared to the STO. When one compares spectra (b) and (d), the graft of Cu(II) on Mo-doped STO recovered this signal, indicating that the paired electrons at the defect moved to the grafted Cu(II) and the unpaired electrons at the oxygen vacancies increased. Then, the decrease of the signal of oxygen vacancy by Mo doping may also be explained by the filling of paired electrons in the vacancy level by doping.

On the UV irradiation with the 360-nm filter, the signal of the trapped electrons was observed at $g = 1.976$ for both STO (spectrum a in Fig. 1) and Cu(II)/STO (spectrum c). When one compares the spectra (c) with (d), it is shown that the signal of the trapped electrons disappeared by Mo doping. Then, the appearance of trapped electron for Cu(II)/STO suggests that the energy level of doped Mo^{6+} is lower than that of Ti^{3+} in STO. The appearance of the trapped electron signal for Cu(II)/STO suggests that the energy level of Ti^{3+} in STO is lower than that of Cu^{2+}/Cu^+ redox. For all the four samples, a large isotropic signal appeared at $g = 2.017$ with UV-light irradiation. This signal is possibly assigned to color center, a kind of lattice vacancy. For Cu(II)/STO (spectrum c), UV irradiation caused larger signal than that observed in STO (spectrum a) with a decrease of

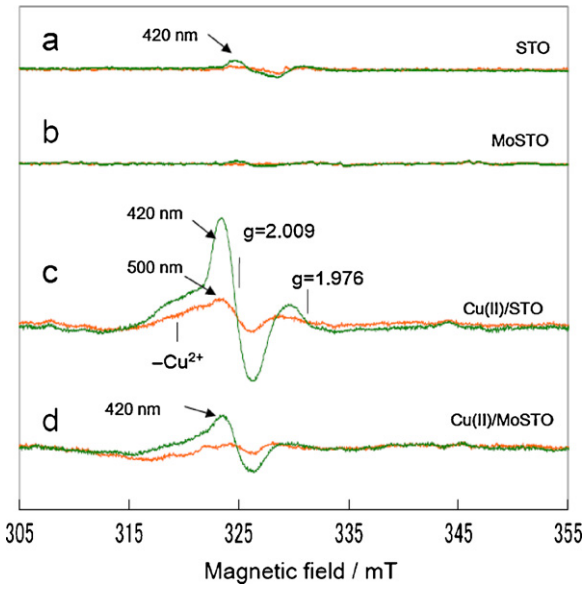

Fig. 2. ESR difference spectra for (a) $SrTiO_3$ and (b) Mo-doped $SrTiO_3$ besides the corresponding Cu(II)-grafted photocatalysts (c and d) showing the effect of visible-light irradiation at the wavelengths longer than 420 nm and 500 nm.

the signal of Cu^{2+}. When one compares spectra (c) and (d) under UV irradiation, the graft of Cu(II) on Mo-doped STO recovered this signal and decreased the Cu^{2+} signal, indicating that the unpaired electrons at the defect moved to the grafted Cu(II) and Cu^{2+} was reduced to Cu^{+}.

Fig. 2 shows the effect of visible light irradiation on the ESR spectra, which are presented as difference spectra against the dark in the expanded magnetic field range (305–355 mT). When Mo-doped STO (spectrum b) was compared with undoped STO (a), the small signal increased on the irradiation of visible light in (a) attributable to trapped holes almost disappeared, indicating that the Mo-doping accelerates the charge recombination although the absorbance in visible-light region was increased [15]. A broad upward signal at 320 mT in the difference spectra (c) shows the decrease of Cu^{2+} by visible light irradiation. The change in the signal intensity of Cu^{2+} corresponds to the IFCT excitation of electrons from valence band of STO to the grafted Cu(II). In the ESR difference spectra (c), the signal of trapped electron appeared at $g = 1.976$ for Cu(II)/STO on the irradiation of visible light (>420 nm). Besides the increase of trapped electrons, the signal of oxygen vacancy ($g = 2.009$) was also increased. On the other hand, the ESR difference spectra (d) for Cu(II)/MoSTO showed that the extent of decrease of the Cu^{2+} signal was smaller than (c), indicating that the excited electrons

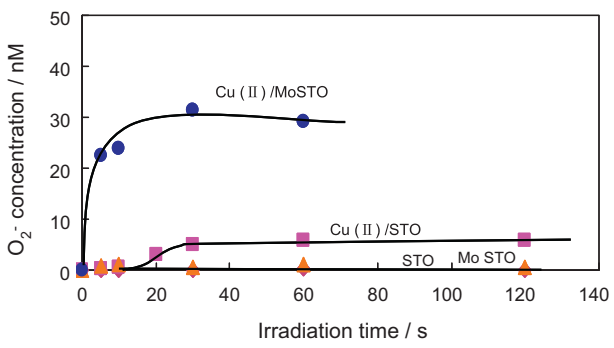

Fig. 3. The concentration of $O_2^{\bullet -}$ produced by the 442-nm irradiation as a function of irradiation time for Cu(II)-grafted Mo-doped $SrTiO_3$ photocatalyst (Cu(II)/MoSTO) and related powders.

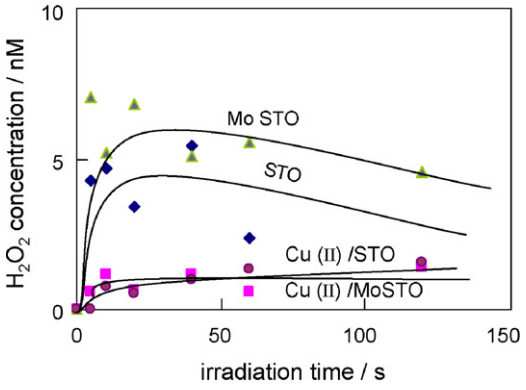

Fig. 4. The concentration of H_2O_2 produced by the 442-nm irradiation as a function of irradiation time for Cu(II)-grafted Mo-doped $SrTiO_3$ photocatalyst and related powders.

at Mo doping levels can not fully move to the grafted Cu(II). The fact that by Mo doping the signal of trapped electrons at $g = 1.976$ was not observed for both UV excitation (Fig. 1(a) and (b), (c) and (d)) and visible light excitation (Fig. 2(c) and (d)) indicates that the Mo-doping level spans under the Ti^{3+} level.

3.2. Chemiluminescence analysis

Fig. 3 shows the formation of $O_2^{\bullet -}$ with visible-light irradiation for the four kinds of STO photocatalysts. By Cu(II)-grafting the formation of $O_2^{\bullet -}$ became detectable. It is notable that Cu(II) grafting on MoSTO produced a large amount of $O_2^{\bullet -}$ while bare MoSTO showed no formation of $O_2^{\bullet -}$. This observation indicates that the energy level formed by Mo doping spans below the $O_2/O_2^{\bullet -}$ redox level. On the other hand, grafted Cu(II) becomes a sink for the electrons excited to higher levels of doped Mo and the formed Cu(I) can reduce O_2 to $O_2^{\bullet -}$. When the amount of $O_2^{\bullet -}$ for Cu(II)/MoSTO is compared with that for Cu(II)/STO, doping with Mo increased the $O_2^{\bullet -}$ formation. This increase reflects the desired increase of the absorbance with the doping of Mo. In the case of Cu(II)/STO, the formation of $O_2^{\bullet -}$ showed some delay by comparison to the case of Cu(II)/MoSTO (Fig. 3). This delay of the reduction of O_2 may be explained by the electron filling in the crystal vacancies which corresponds to the large ESR difference signal observed at $g = 2.009$ (Fig. 2(c)) on the visible-light irradiation.

Fig. 4 shows the amount of H_2O_2 as a function of irradiation time. The amount of formed H_2O_2 was few nM, which is extremely smaller than that for Cu(II)-deposited WO_3 (ca. 200 nM) [24]. In the case of TiO_2 photocatalysts, the formed H_2O_2 was adsorbed on TiO_2 surface and became undetectable with

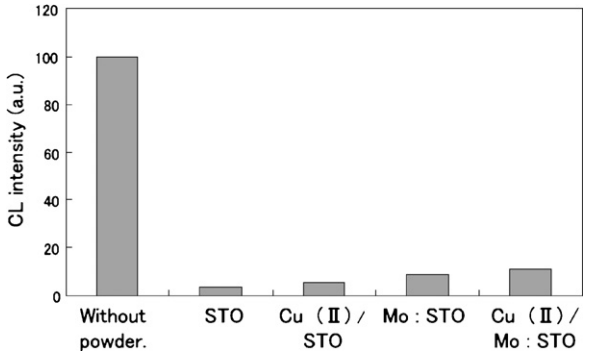

Fig. 5. Relative intensities of chemiluminescence for 1 μM H_2O_2 and 0.1 mM luminol with hemoglobin (Hb). The effect of powders of modified $SrTiO_3$ was tested by adding the presented powders 15 min before the addition of Hb.

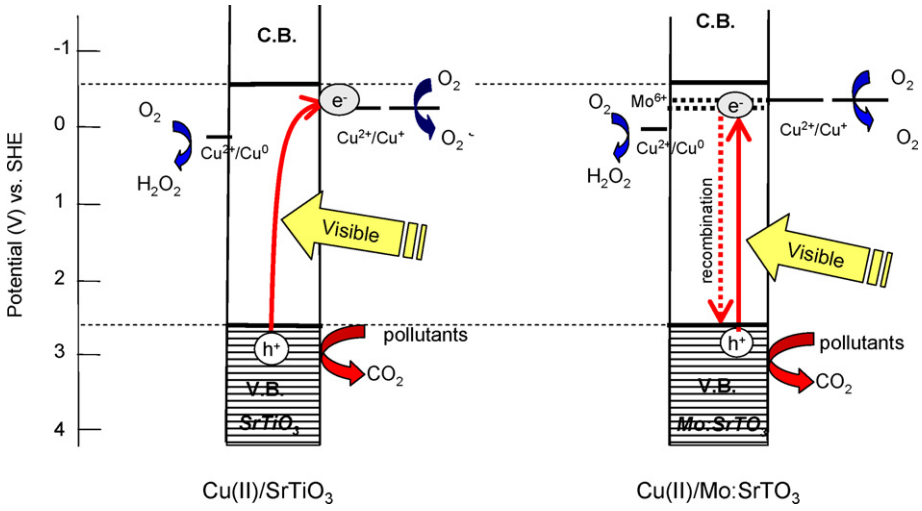

Fig. 6. Energy diagram of Cu(II)-grafted $SrTiO_3$ and Cu(II)-grafted Mo-doped $SrTiO_3$ photocatalysts at pH 7, showing the paths of photoexcited electron and hole suggested by the present study.

chemiluminescence photometry. In order to know the adsorption of H_2O_2 on the surface of STO particles, the decrease of H_2O_2 in solution was measured under dark condition. In the optical cell, 1 μM H_2O_2 and 0.1 mM luminol were placed and the chemiluminescence intensity on the addition of Hb was measured without irradiation. When each photocatalyst powder was added 15-min before the Hb addition, the chemiluminescence intensity for H_2O_2 decreased as shown in Fig. 5 for each photocatalyst powder. Although some adsorption was observed, H_2O_2 can be detected with STO powders in solution (Fig. 5). Then, it may conclude that the amount of produced H_2O_2 by the visible light excitation was very small. Accordingly the formed H_2O_2 was rapidly reduced to H_2O or decomposed into O_2 and H_2O. The decomposition of H_2O_2 at grafted Cu(II) was supported by the fact that the formation of H_2O_2 was smaller than the non-deposited samples as shown in Fig. 4, though the formation of $O_2^{\bullet-}$ was increased.

3.3. Reaction mechanism of the modified $SrTiO_3$ photocatalyst

Based on the experimental results and the above discussions, the mechanism of photocatalytic reactions on visible-light irradiation is illustrated in Fig. 6 for Cu(II)/STO and Cu(II)/MoSTO besides the potential energy at pH 7. The potential levels of the energy band for $SrTiO_3$ are similar to those of anatase TiO_2 [15]. By the Mo-doping, visible light can be absorbed with the electron excitation from valence band of $SrTiO_3$ to the Mo doping levels. Since without Cu(II) grafting no $O_2^{\bullet-}$ was detected for MoSTO on 442-nm irradiation, the lowest Mo-doping level is lower than that of the $O_2/O_2^{\bullet-}$ redox level. The detection of $O_2^{\bullet-}$ for the Cu(II)-grafted STO sample (Fig. 3) indicates that Cu^{2+}/Cu^{+} redox level of the grafted Cu(II) locates near $O_2/O_2^{\bullet-}$ at neutral pH similarly to the case of TiO_2 [24]. By Mo doping in $SrTiO_3$, the excited electrons in the Mo-doping levels are trapped in Cu(II) and reduce O_2 to $O_2^{\bullet-}$ more effectively than the case of undoped $SrTiO_3$, while the visible-light can also be absorbed by interfacial charge transfer from valence band to the deposited Cu(II). In the ESR experiment for Mo-doped photocatalysts, the signal decrease for Cu^{2+} was small (Fig. 2(d)) and the signal of the lattice vacancy ($g = 2.009$) became also small with the doping. This observation suggests that the electrons produced at the Mo-doping levels by visible-light excitation tend to recombine with the holes produced at the valence band of $SrTiO_3$, but the grafting of Cu(II) species drastically retards the recombination.

4. Conclusions

In the present experiment, by detecting reaction intermediates, trapped holes, trapped electrons, $O_2^{\bullet-}$, and H_2O_2, the reaction mechanism of visible light responsive Cu(II)-deposited Mo-doped $SrTiO_3$ photocatalyst was clarified. The concept of designing for increasing photon absorption was supported by these observations. However, the existence of lattice vacancy was observed in the ESR measurements and the electron–hole recombination is expected for the Mo-doped $SrTiO_3$ photocatalysts. Though the basic mechanism for the modified $SrTiO_3$ has been shown in the previous report [15], a detailed mechanism presented here should provide useful knowledge for designing new visible responsive photocatalysts.

Acknowledgements

This work was performed under the management of the Project to Create Photocatalyst Industry for Recycling-Oriented Society, supported by the New Energy and Industrial Technology Development Organization (NEDO) in Japan.

References

[1] M.R. Hoffmann, S.T. Martin, W. Choi, D.W. Bahnemann, Chem. Rev. 95 (1995) 69–96.
[2] M. Kaneko, I. Ohkura (Eds.), Photocatalysis, Kodansha-Springer, Tokyo, 2002.
[3] A. Fujishima, X. Zhang, D. Tryk, Surf. Sci. Rep. 63 (2008) 515–582.
[4] M.A. Henderson, Surf. Sci. Rep. 66 (2011) 185–297.
[5] S. Sato, Chem. Phys. Lett. 123 (1986) 126–128.
[6] R. Asahi, T. Morikawa, T. Ohwaki, K. Aoki, Y. Taga, Science 293 (2001) 269–271.
[7] H. Irie, Y. Watanabe, K. Hashimoto, J. Phys. Chem. B 107 (2003) 5483–5486.
[8] Y. Nosaka, M. Matsushita, J. Nishino, A. Nosaka, Sci. Technol. Adv. Mater. 6 (2005) 143–148.
[9] T. Umebayashi, T. Yamaki, H. Ito, K. Asahi, Appl. Phys. Lett. 81 (2002) 454–456.
[10] T. Ohno, T. Mitsui, M. Matsumura, Chem. Lett. 32 (2003) 364–365.
[11] Y. Murakami, B. Kasahara, Y. Nosaka, Chem. Lett. 36 (2007) 330–331.
[12] T. Arai, M. Horiguchi, M. Yanagida, T. Gunji, H. Sugihara, K. Sayama, J. Phys. Chem. C 113 (2009) 6602–6609.
[13] Y. Kuroda, Y. Hosogi, M. Sanbayashi, Photocatalysis 33 (2008) 188–189 (in Japanese).
[14] H. Irie, S. Miura, K. Kamiya, K. Hashimoto, Chem. Phys. Lett. 457 (2008) 202–205.
[15] X. Qiu, M. Miyauchi, H. Yu, H. Irie, K. Hashimoto, J. Am. Chem. Soc. 132 (2010) 15259–15267.

[16] W. Choi, A. Termin, M.R. Hoffmann, J. Phys. Chem. 98 (1994) 13669–13679.
[17] H. Yamashita, M. Harada, J. Misaka, M. Takeushi, M. Anpo, J. Photochem. Photobiol. A 148 (2002) 257–261.
[18] H. Yu, H. Irie, K. Hashimoto, J. Am. Chem. Soc. 132 (2010) 6898–6899.
[19] Y. Nosaka, Y. Yamashita, H. Fukuyama, J. Phys. Chem. B 101 (1997) 5822–5827.
[20] T. Hirakawa, Y. Nosaka, Langmuir 18 (2002) 3247–3254.
[21] T. Hirakawa, Y. Nosaka, J. Phys. Chem. C 112 (2008) 15818–15823.
[22] Y. Nakaoka, Y. Nosaka, J. Photochem. Photobiol. A 110 (1997) 299–307.
[23] A.A. Altynnikov, L.T. Tsikoza, V.F. Anufrienko, J. Struct. Chem. 47 (2006) 1161–1169.
[24] Y. Nosaka, S. Takahashi, H. Sakamoto, A. Nosaka, J. Phys. Chem. C 115 (2011) 21283–21290.